Published in final edited form as:
J Immunol. 2010 January 15; 184(2): 975–983. doi:10.4049/jimmunol.0900650.

SURFACTANT PROTEIN B PROPEPTIDE CONTAINS A SAPOSIN-LIKE PROTEIN (SAPLIP) DOMAIN WITH ANTIMICROBIAL ACTIVITY AT LOW pH*

Li Yang[†], **Jan Johansson**[‡], **Ross Ridsdale**[†], **Hanna Willander**[‡], **Michael Fitzen**[‡], **Henry T. Akinbi**[†], and **Timothy E. Weaver**[†]

[†] Division of Pulmonary Biology, Cincinnati Children's Hospital Medical Center and University of Cincinnati College of Medicine, Cincinnati, Ohio

[‡] Department of Anatomy, Physiology and Biochemistry, The Biomedical Centre, Swedish University of Agricultural Sciences, Uppsala, Sweden

Abstract

Surfactant protein B (SP-B) proprotein contains 3 saposin-like protein (SAPLIP) domains: A SAPLIP domain corresponding to the mature SP-B peptide is essential for lung function and postnatal survival; the function of SAPLIP domains in the N-terminal (SP-B^N) and C-terminal (SP-B^C) regions of the proprotein are not known. In the current study, SP-B^N was detected in the supernatant of mouse bronchoalveolar lavage fluid (BALF) and in non-ciliated bronchiolar cells, alveolar type II epithelial cells and alveolar macrophages. Recombinant SP-B^N indirectly promoted uptake of bacteria by macrophage cell lines and directly killed bacteria at acidic pH, consistent with a lysosomal, antimicrobial function. Native SP-B^N isolated from BALF also killed bacteria, but only at acidic pH; the bactericidal activity of BALF at acidic pH was completely blocked by SP-B^N antibody. Transgenic mice overexpressing SP-B^N and mature SP-B peptide had significantly decreased bacterial burden and increased survival following intranasal inoculation with bacteria. These findings support the hypothesis that SP-B^N contributes to innate host defense of the lung by supplementing the non-oxidant antimicrobial defenses of alveolar macrophages.

Keywords

Infection-bacterial; Animals-rodent; Tissues-lung

INTRODUCTION

Pulmonary surfactant is a mixture of lipids and proteins synthesized and secreted by type II epithelial cells into the alveolar spaces where it forms a film at the air-liquid interface. The phospholipid components of the surfactant film promote alveolar stability by preventing collapse during deflation and facilitating alveolar expansion during inflation. Surfactant proteins, in particular surfactant protein B (SP-B), promote the formation and maintenance of a stable phospholipid-rich surface film. Mice deficient in SP-B succumb to acute respiratory failure (1,2); similarly, human infants with *SFTPB* mutations that lead to loss of peptide in the airspaces, die of respiratory distress syndrome in the postnatal period (3,4). It is likely that the

*This research was supported by a grant from the National Heart, Lung and Blood Institute (HL56285)

Correspondence: Timothy E. Weaver, Ph.D., Cincinnati Children's Hospital Medical Center, Division of Pulmonary Biology, MLC 7029, 3333 Burnet Avenue, Cincinnati, OH 45229-3039, Phone: (513) 636-7223, FAX: (513) 636-7868, tim.weaver@cchmc.org.

membranolytic properties of SP-B play an important role in modulating the structure and function of surfactant in the postnatal lung (5–8).

SP-B belongs to the saposin-like (SAPLIP) family of proteins that include 235 different members (9,10). The defining feature of SAPLIPs is 6 conserved cysteines that form three intramolecular disulfide bridges. The bridge structure stabilizes a "saposin-fold," composed of 4–5 amphipathic helices, that facilitates transient or permanent interaction with membranes (11). The index member of this family, prosaposin, contains 4 saposin domains; proteolytic processing of the proprotein yields 4 saposin peptides each approximately 80 amino acids in length, that act as co-factors in lysosomal degradation of sphingolipids. Like prosaposin, SP-B is synthesized as a proprotein (proSP-B) that contains three saposin-like domains (Fig. 1A). Processing of proSP-B to the mature peptide that is secreted with surfactant lipids is well characterized (12,13). The N-terminal propeptide of SP-B (residues 31-191, Fig. 1A) plays a critical role in the intracellular trafficking of the hydrophobic, mature peptide (SP-B, Fig. 1A); in addition, the propeptide encodes a saposin-like domain of unknown function (SP-B^N,Fig. 1A). The C-terminal domain of proSP-B (SP-B^C,Fig. 1A) encodes a third saposin-like domain, also of unknown function. Unlike the mature peptide and SP-B^C, SP-B^N is not a cationic peptide. In this regard, SP-B^N resembles the amoebapores, a subgroup of saposin-like peptides with cytolytic and antimicrobial properties (10,14). The current study was designed to test the hypothesis that SP-B^N is a component of innate host defense of the lungs.

MATERIALS AND METHODS

Expression, purification and refolding of recombinant mouse SP-B^N

SP-B^N cDNA (encoding residues 61-146, Fig. 1A) was generated from mouse type II cell RNA by RT-PCR using upstream primer 5′-GGG AAT TCC ATA TGC ATG CAG GAG CTA ATG ACC TG-3′ and downstream primer 5′-CCG CTC GAG CTG CCC ACG TGG GCA CAG GCC-3′; restriction sites for Nde I and Xho I were encoded in the upstream and downstream primers respectively. The amplified 258 bp fragment was cloned into the Nde I/Xho I sites of PET21a vector (Novagen, Madison, WI). SP-B^N was expressed in *E. coli* BL21 (DE3). Transformed bacteria were grown in LB (Luria-Bertani) medium supplemented with 50 μg/ml carbenicillin to an OD_{600} of 0.6 and protein expression induced by addition of 0.1 mM IPTG for 3h at 37°C. 10–20% Tricine-SDS PAGE of bacterial lysates expressing SP-B^N detected a band, Mr = 9000, following IPTG induction. The broth was centrifuged and the isolated bacterial pellet lysed by sonication in 20 mM Tris buffer, pH 7.4, 4°C. Inclusion bodies were recovered by centrifugation, washed in Tris buffer and solubilized in 20 mM Tris, 6 M Urea, 50 mM DTT buffer, pH 7.4. Denatured, solubilized inclusion body protein was diluted (1:10) in 20 mM Tris, 6 M urea, 0.5 M NaCl, 3 mM reduced glutathione, 0.3 mM oxidized glutathione, pH 7.4, and dialyzed three times against 10 volumes of the same buffer in which urea concentration was reduced to 2 M followed by dialysis against 10 volumes of 20 mM Tris, 0.5 M NaCl (Ni-NTA binding buffer), pH 7.9. After centrifugation, the supernatant was applied to a Ni-NTA agarose column (Novagen). The column was washed and eluted according to the manufacturer's protocol. Eluted protein was dialyzed against sodium phosphate buffer, pH 7.0, and stored in aliquots at −80°C.

Circular dichroism (CD) experiments

CD spectra in the far-UV region (250–190 nm) were recorded at 25 °C with a Jasco J-810–150S spectropolarimeter (Jasco, Tokyo, Japan) using a bandwidth of 1 nm and a response time of 2 s; 10 data points/nm were collected. Each spectrum shown is the average of three scans. The residual molar ellipticity (θ) is expressed in kdeg × cm^2 × $dmol^{-1}$. Spectra were recorded of 25 μM SP-B^N in PBS pH 7.4 or in 20 mM NaAc pH 5.6 with or without 100 μM 1-Palmitoyl-sn-glycero-3-phosphocoline (lysoPC, Sigma-Aldrich, Germany).

Trypsin digestion and identification of disulfides

50 μg SP-B^N was treated with 500 ng trypsin (Promega, Madison, WI, USA) in a 50 mM Tris buffer, pH 8.0, containing 2 M Urea at 37 °C for 3 hours. The reaction was stopped by the addition of trifluoroacetic acid (10% in final concentration). The Urea-containing buffer was changed to a 50 mM ammonium bicarbonate buffer, pH 7.4. Digested SP-B^N was reduced by boiling in 1% β-mercaptoethanol (Sigma, St. Louis, MO, USA) and desalted prior to MS analysis with C_{18} ZipTips (Millipore, Billerica, MA, USA) according to the manufacturer's instructions. Peptides were eluted in 75% acetonitrile, 0.1% formic acid directly onto the MALDI target and mixed with α-cyano (Bruker Daltonics, Bremen, Germany) matrix. MALDI-MS spectra were acquired on a PerSeptive Biosystems Voyager-DE Pro mass spectrometer (Applied Biosystems, Foster City, CA, USA) operated in reflector mode and analyzed using the PerSeptive Data Explorer 3.4.0 software package.

For LC-MS, digested SP-B^N was reduced by incubation in 5 mM dithiothreitol (Sigma, St. Louis, MO, USA) for 60 min at 37°C and carbamidomethylated by addition of iodoacetamide (Sigma, St. Louis, MO, USA) to a final concentration of 7mM and incubation for 15 min in the dark at 20°C.

ESI-MS and MS/MS data were acquired on a QTOF Premier API instrument (Waters, Manchester, UK) equipped with the standard Z-spray source and a nanoAcquity nanoflow LC system. Lockmass reference of (Glu1)fibrinopeptide (Sigma, St. Louis, MO, USA) was used for mass scale correction.

SP-B^N antibody

Recombinant SP-B^N was injected into guinea pigs to generate polyclonal antibodies. SP-B^N antibodies were initially characterized by western blotting of lung homogenates from E18.5 *Sftpb*$^{-/-}$ mice and WT littermates. The antibody used in the current study detected a single protein, Mr = 8000, in WT mice and no protein bands in SP-B knock out mice (data not shown and Fig. 5A, right panel, lane 2). All experiments involving the use of animals (guinea pigs, mice, and rats) were approved by the Institutional Animal Care and Use Committee at the Cincinnati Children's Research Foundation.

Isolation of native rat SP-B^N

BALF was collected from rats as previously described (15). BALF was centrifuged at 5000 × g for 30 min and supernatant from 10 rats pooled. The concentrated sample was dialyzed against distilled water at 4°C for 16 h; 2% BioLyte ampholytes (Bio-Rad Laboratories, Hercules, CA), pH range 3–10, were added and preparative isoelectric focusing performed (IEF, Rotofor, Bio-Rad Laboratories). Twenty fractions were harvested and analyzed by 10–20% Tricine-SDS PAGE and Imperial blue staining (Pierce) or western blotting using SP-B^N antibody. Rotofor fractions containing SP-B^N were combined, concentrated by vacuum centrifugation and further fractionated by size exclusion chromatography (Zorbax GF250, Agilent Technologies). HPLC fractions containing SP-B^N were combined, concentrated and analyzed by Mass Spectrometry (University of Cincinnati, MS core) and Edman degradation (Biosynthesis, Lewisville, TX).

Identification endogenous mouse SP-B^N

Mice were lavaged and the supernatant, cell pellet and surfactant pellet analyzed by 10–20% tricine-SDS PAGE followed by western blotting. SP-B^N antibody was used at a dilution of 1:5000 and immunoreactive protein visualized by enhanced chemiluminescence (Pierce) followed by exposure to Kodak X-Omat AR film.

For immunohistochemical analyses, lungs from 5-wk-old WT mice were inflation-fixed and immunohistochemistry performed as previously described (16). Immunostaining for SP-B^N

was performed at an antibody dilution of 1:2500. Parallel lung sections were incubated with preimmune guinea pig serum to verify the specificity of immunostaining.

Bacteria

Heat-killed S*taphylococcus aureus* (*S. aureus*) fluorescently labeled with Alexa Fluor 594 were purchased from molecular probes (Eugene, OR). Bioluminescent *Pseudomonas aeruginosa* (*P. aeruginosa*) Xen 5 were purchased from Caliper LifeScience. *Klebsiella pneumoniae* (*K. pneumoniae*) strain K2 (from Dr. Korfhagen, Cincinnati Children's Hospital, Cincinnati, OH) and a clinical isolate of *S. aureus* were also used in the current study. To minimize variability in virulence, all bacteria were selected from aliquots of the same passage stored at −70°C in 20% glycerol/PBS. For each experiment, an aliquot of bacteria was thawed and plated on tryptic soy/5% sheep blood agar. A single colony was inoculated into 4 ml of LB medium (*P. aeruginosa*, *K. pneumoniae*) or brain-heart-infusion medium (*S. aureus*) and grown to late log phase. Bacteria were pelleted from the medium by centrifugation at 500 × g for 10 min, washed in sterile PBS, and resuspended in 4 ml of sterile PBS. For each experiment, the concentration of bacteria was determined by quantitative culture on sheep blood agar plates.

Analyses of recombinant SP-B^N activity

For phagocytosis assays, RAW264.7 macrophages were maintained as described by Vunta et al., (17). Cells were seeded at 1×10^5/ml (3ml total volume) on cover slips in 6-well plates, and incubated with heat-killed *S. aureus* fluorescently labeled with Alexa Fluor 594 (MOI =50) with or without recombinant SP-B^N or heat-denatured SP-B^N (recombinant SP-B^N was heated at 100°C for 1 h in 1% β-mercaptoenthanol). Non-internalized particles were removed by extensive washing with PBS, and cells were fixed in PBS containing 4% paraformaldehyde at 25 °C for 15 min and evaluated by fluorescence microscopy as previously described by Shibata et al., (18).

Recombinant mouse SP-B^N was labeled with FITC according to the manufacturer's protocol (PIERCE). Briefly, 40μl reconstituted FITC was added to 200 μg recombinant SP-B^N in 50mM Borate buffer, pH8.5 at RT for 1h. Unconjugated fluorescent dye was removed by dialysis against PBS in the dark.

To assess bacterial uptake and killing, RAW264.7 cells were incubated with recombinant SP-B^N in antibiotic-free RPMI 1640/FBS in a volume of 1 ml. After washing with antibiotic-free RPMI 1640, cells were infected with 2×10^6 *S. aureus or K. pneumoniae*. Infected monolayers were washed with warm PBS twice, and incubated with RPMI 1640 containing 100μg/ml carbenicillin or gentamycin to kill extracellular *S. aureus and K. pneumoniae*, respectively. Intracellular bacteria were released at 1, 2, 4, 6 and 24 h post-infection by lysing cells in 1% Triton X-100 and the number of live bacteria at each time point assessed by quantitative culture.

To assess the bacteriostatic property of recombinant SP-B^N, 10^3 CFU of *K. pneumoniae* or *S. aureus* were resuspended in sterile 100 μl of PBS, pH 7.0, or 2 mM sodium acetate buffer, pH 5.6. Serial dilutions of recombinant SP-B^N were added to individual wells in triplicate and incubated for 3h at 37°C with rocking. Direct bactericidal activity of recombinant SP-B^N was assessed using fluorescent probes Syto9 and propidum iodide (Molecular Probes) at concentrations of 6 μM and 30 μM, respectively. Bacteria were subsequently dispersed and aliquots were plated on blood agar for quantitative culture. Viable pathogen counts after SP-B^N treatment were determined from the number of colonies obtained on the control plates (0 μM SP-B^N) compared with the number of colonies from SP-B^N -treated samples.

To assess binding of SP-B^N to lipid membranes, 10 μg of recombinant SP-B^N was incubated with mouse BALF containing surfactant lipids or *S. aureus* (10^5 CFU) in 0.3 ml of 2 mM

sodium acetate (pH 5.6) or PBS (pH 7.4) at RT for 2 h. The mixture was centrifuged at 15000 × g for 30 min to separate supernatant and pellet. The supernatant was concentrated by vacuum centrifugation to decrease the volume and supernatant and pellet were analyzed by 10–20% Tricine-SDS PAGE followed by western blotting.

Analyses of native SP-B^N activity

BALF was collected from wild type mice. The mouse trachea was cannulated and the lungs were washed 3 times with 1 ml of PBS. BALF was immediately centrifuged and the supernatants from 5 mice pooled and concentrated to assess SP-B^N bactericidal activity. 1×10^7 CFU *P. aeruginosa* Xen 5 were suspended in 200 μl of PBS (pH 7.4) or 2 mM sodium acetate (pH 5.6) and incubated overnight at 37°C with BALF supernatant +/− SP-B^N IgG antibody or BALF and SP-B^N IgG antibody +/− recombinant SP-B^N in triplicate in a 96-well plate. The number of viable bacteria was assessed by measuring luminescence. Results are expressed as percent viable bacteria = 100 × (relative light units from control wells (without treatments) − relative light units from experimental wells)/relative light units from control wells.

We have previously described the generation of transgenic mice that express truncated human SP-B (SP-B$^{\Delta C}$) (19). hSP-B$^{\Delta C}$/mSP-B$^{+/+}$ (transgenic mice) overexpress the N-terminal propeptide and mature peptide of SP-B (Fig. 5A). Transgenic and WT mice were intranasally inoculated with 3.7×10^7 CFU *P. aeruginosa* Xen 5 in 50 μl of PBS, as previously described (20). *In vivo* bioluminescent images were acquired under anesthesia with the IVIS system (Caliper LifeSciences) at 1, 8, and 24 h following infection. Images were acquired with a 20 cm field of view and an exposure time of 20s (data not shown). The experiments were repeated 3 times and data pooled.

Transgenic and WT mice were also challenged with *S. aureus* and analyzed at 24, or 48 h postinfection. Lungs were weighed, homogenized, and equal amounts of protein plated for quantitative culture. The numbers of colonies were expressed as CFU per gram of lung tissue. Studies were conducted three times (n = 9–10 mice/group) and results pooled.

To assess survival, transgenic and WT mice (n = 16 mice/group) were intranasally inoculated with either 3.7×10^7 CFU *P. aeruginosa* Xen 5 or 5×10^8 CFU *S. aureus* suspended in 50 μl of PBS. Water and food were provided ad libitum during the period of observation. The number of surviving mice was documented every 12 h for up to 120 h, at which time surviving mice were sacrificed.

Statistical Analysis

All data are expressed as mean ± SEM. Difference between groups was analyzed by one-way analysis of variance, and post-hoc testing for pairwise group differences was conducted using the Student-Newman-Keuls test. Non-parametric survival distribution was estimated to examine the differences in survival among groups and was subsequently analyzed using Kaplan-Meier curve statistics. The differences between the groups of mice were assessed using log-rank test.

RESULTS

Identification and localization of SP-B^N in mouse lung

Based on alignment of SP-B with other members of the SAPLIP family of proteins (not shown), the region encoding the predicted mouse N-terminal saposin domain (SP-B^N, residues 61-146, Fig. 1A) was subcloned into pET21 with a C-terminal histidine tag. 10–20% Tricine SDS-PAGE of bacterial lysates expressing SP-B^N detected a band, Mr = 9000, following IPTG

induction (not shown). Recombinant mouse SP-B^N was purified from inclusion bodies by denaturing, Ni-NTA affinity chromatography, refolded and dialyzed. 10–20% Tricine-SDS PAGE of purified recombinant SP-B^N and Imperial blue staining (Pierce) indicate that the recombinant SP-B^N is >90% pure (Fig. S1). CD analyses indicated that recombinant SP-B^N contained mainly α-helical structure, which did not change significantly at different pH values or in the presence of lysoPC (Fig. S2). The results are summarized in Supplemental Table 1 and agree with a predicted saposin-like fold of SP-B^N. Recombinant SP-B^N was digested with trypsin and reduced and nonreduced peptides analyzed by ESI-MS/MS. The results are summarized in Supplemental Table 2. To identify disulfide links between tryptic fragments of SP-B^N, the digested recombinant protein was analyzed by MALDI-MS under reducing and non-reducing condition (Fig. S3). The identity of the peaks corresponding to disulfide-linked and reduced peptides was verified by LC-MS/MS (Fig. S4). The results of these analyses were consistent with three disulfide bonds in which the two centrally located cysteines form a bridge and the two cysteines at the N-terminal form bridges with the two cysteines at the C-terminal. This pattern is similar to that reported for the mature SP-B peptide (21,22). Overall, these experiments suggest that recombinant SP-B^N assumes a saposin-like fold that is stabilized by three disulfide bridges.

Recombinant SP-B^N was injected into guinea pigs to generate polyclonal antibodies. SP-B^N antibody detected a protein, Mr = 8000, in the supernatant from mouse BALF under non-reducing electrophoretic conditions (Fig. 1B, lane 3); a minor band, Mr = 16000, consistent with a SP-B^N dimer was also detected. Only a very small amount of SP-B^N was associated with surfactant lipids isolated from BALF (Fig. 1B, lane 5). No immunoreactive bands were detected in liver homogenate (Fig. 1B, lane 2) and the antibody did not cross-react with human SP-B (Fig. 5A, right panel, lane 2). The increased electrophoretic mobility of endogenous mouse SP-B^N relative to recombinant peptide suggested that the saposin-like domain was smaller than predicted (Fig. 1A). In order to establish the NH_2-terminus of endogenous SP-B^N, Rat BALF supernatant was concentrated and subjected to preparative IEF followed by analytical size exclusion HPLC and SDS-PAGE. Edman degradation identified alanine at position 62 as the N-terminal residue (Fig. 1C, first amino acid in the lower line). Trypsin digestion and MS/MS analyses of purified rat SP-B^N yielded 7 peptides (covering 78% of SP-B^N) that all mapped within the predicted saposin-like domain (Fig. 1C, lower line). Taking into account the larger size of recombinant SP-B^N (which includes an N-terminal histidine and 6 C-terminal histidines not present in the endogenous peptide), the strict conservation of the 6-cysteine residues in SAPLIP family members, the identification of Ala^{62} as the N-terminal residue and an estimated mass of 8kDa, it is likely that Cys^{142} represents the C-terminus of endogenous mouse SP-B^N (Fig. 1C, upper line).

Immunohistochemical analyses of lung sections with SP-B^N antibody detected staining in nonciliated bronchiolar epithelial cells (Clara cells) and alveolar type II epithelial cells, which could represent proSP-B and/or SP-B^N (Fig. 1D, upper panels). Strong immunoreactivity was detected in macrophages, both in uninfected lungs and 24 h following challenge with *S. aureus* (Fig. 1D, right panels). SP-B^N, Mr =8000, was the only form of SP-B detected in cells and BALF supernatant isolated from the airspaces of uninfected and infected mice (Fig. 1E).

Recombinant SP-B^N enhances uptake and killing of bacteria in vitro

Localization of endogenous SP-B^N to alveolar macrophages (Fig. 1D) suggested that the peptide might facilitate uptake and/or intracellular killing of bacteria by alveolar macrophages. This hypothesis was initially tested *in vitro* by incubating heat-killed fluorescent-labeled *S. aureus* with recombinant SP-B^N prior to incubation with primary mouse lung macrophages or the mouse macrophage cell line RAW 264.7. Phagocytosis after 1 hr was not increased compared to untreated bacteria suggesting that SP-B^N did not directly promote uptake of

bacteria (not shown). In contrast, pre-incubation of macrophages (not shown) or RAW264.7 (Fig. 2A) cells with recombinant SP-B^N for 1 hr prior to addition of bacteria resulted in a dramatic increase in intracellular *S. aureus*; similar results were observed in MHS cells, a mouse alveolar macrophage cell line (not shown). Heat-inactivation of recombinant SP-B^N blocked the increase in uptake of *S. aureus* (not shown). FITC-labeled, recombinant SP-B^N co-localized with internalized, heat-killed *S. aureus* (Fig. 2B) and with the lysosomal marker Lamp-1 (not shown). Colocalization of SP-B^N with internalized bacteria suggested that SP-B^N might play a role in intracellular killing of pathogens. To test this hypothesis, RAW264.7cells were incubated with recombinant SP-B^N for 1h prior to incubation with *S. aureus* or *K. pneumoniae* for 1–24 h. Quantitative culture of cell lysates 24h later indicated that bacterial killing was significantly increased (Fig. 2C). Taken together, these data suggest that SP-B^N indirectly promotes uptake of bacteria and facilitates intracellular killing.

Recombinant SP-B^N directly kills bacteria at low pH

In order to determine if SP-B^N directly killed bacteria, *S. aureus* was incubated with recombinant SP-B^N for 90 min and stained with Syto9 (stains living bacteria green) and propidium iodide (stains dead/dying bacteria red). Fluorescence microscopy detected a dose-dependent increase in propidium iodide staining in SP-B^N-treated samples at pH5.6 but not at pH7.4 (Fig. 3A), consistent with killing in a lysosomal compartment. Subsequently, clinical isolates of *K. pneumoniae* or *S. aureus (*10^3 CFU) were incubated with recombinant SP-B^N for 3 hrs at pH 5.6 (Fig. 3B) or pH 7.4 (not shown). Recombinant SP-B^N exhibited antimicrobial activity against both Gram-positive and Gram-negative organisms at pH 5.6 but not pH 7.4. At 0.5 μM SP-B^N, growth inhibition of *K. pneumoniae* and *S. aureus* was >50%. *K. pneumoniae* or *S. aureus* (10^3 CFU) were also incubated with purified native rat SP-B^N (native refers to endogenous SP-B^N isolated from rat BALF) for 3 hrs at pH 5.6 (Fig 3C) or pH 7.4 (not shown). Native SP-B^N inhibited growth of both bacteria but was more effective against *K. pneumoniae* (> 50% inhibition at 0.1 μM native SP-B^N).

Since all members of the SAPLIP family are stably or transiently associated with lipids, experiments were designed to determine if recombinant SP-B^N associated with surfactant. Recombinant SP-B^N was added to mouse BALF at pH 5.6 or pH 7.4, incubated at RT for 2 h then centrifuged to separate surfactant lipids and supernatant. Recombinant SP-B^N was recovered in the surfactant pellet at pH 5.6 but not at pH 7.4 (Fig. 3D). Experiments were then designed to determine if recombinant SP-B^N directly bound to bacterial membranes. Recombinant SP-B^N was added to *S. aureus* at pH 5.6 or pH 7.4, incubated at RT for 2 h then centrifuged to separate the bacterial pellet and supernatant. Most SP-B^N was recovered in the bacterial pellet at pH 5.6; binding of recombinant peptide to bacteria was much reduced at pH 7.4 (Fig. 3E). Taken together, these data suggest that SP-B^N associates with bacterial membranes at low pH and directly facilitates intracellular killing.

Endogenous SP-B^N inhibits bacterial growth

The results of experiments with recombinant SP-B^N (Figs. 2 and 3) suggested that endogenous SP-B^N might play an important role in host defense of the lungs. The ability of native SP-B^N to inhibit bacterial growth was tested by incubating bioluminescent *P. aeruginosa* Xen 5 (Caliper Life Sciences) with increasing amounts of mouse BALF supernatant (adjusted to pH 5.6 or pH 7.4) at 37°C, overnight. Dose-dependent inhibition of bacterial growth was detected at acidic pH, (Fig. 4A) but not pH 7.4 (not shown). To confirm that this effect was related to endogenous SP-B^N, anti-mouse SP-B^N IgG was added to BALF prior to incubation with bacteria. Addition of SP-B^N antibody directly to the bacterial suspension in the absence of BALF did not inhibit growth of *P. aeruginosa* (Fig. 4B); in fact, both SP-B^N IgG (Fig 4B) and irrelevant IgG (Fig 4C) increased bacterial growth. In the presence of BALF, bacterial growth was significantly inhibited and this effect was blocked by prior incubation of BALF with SP-

B^N antibody (Fig. 4B). Incubation of SP-B^N IgG with recombinant SP-B^N partially reversed the inhibitory effects of SP-B^N antibody (Fig. 4C). Taken together, these data support the hypothesis that native SP-B^N inhibits bacterial growth at acidic pH. However, because of the higher than expected numbers of bacteria in the presence of SP-B^N IgG, we cannot exclude the possibility that the antibody also inhibits some other antimicrobial component in the BALF.

Increased expression of SP-B^N in transgenic mice enhances survival and bacterial clearance following infection with P. aeruginosa

In order to confirm the role of SP-B^N in host defense *in vivo*, we used transgenic mice that express a truncated form of human proSP-B (SP-$B^{\Delta C}$ i.e. the entire region of the SP-B proprotein that is C-terminal to the mature peptide was deleted, see Fig. 1A) in the WT mouse background (hSP-$B^{\Delta C}$/mSP-$B^{+/+}$). We previously showed that mature SP-B peptide in lung homogenates of these transgenic mice is elevated 2–3 fold (19). Western blots, using an antibody that detected both human and mouse SP-B^N, detected a similar increase in SP-B^N concentration in BALF (Fig. 5A, left panel, compare lanes 1 and 3). Endogenous SP-B^N in transgenic mice was not increased indicating that elevated SP-B^N concentration was related to transgene expression (Fig. 5A, right panel, compare lanes 1 and 3). To assess the impact of increased SP-B^N on bacterial killing *in vivo*, WT and transgenic mice were intranasally inoculated with 3.7×10^7 CFU of bioluminescent *P. aeruginosa* Xen 5. Three WT animals died before acquisition of bioluminescence at 24 h. Quantitation of bioluminescence indicated that bacterial burden was significantly decreased in transgenic mice at 8 and 24 h postinfection (Fig. 5B), consistent with a protective effect of SP-B^N. Survival studies indicated that all WT mice died by 48 h postinfection whereas only 20% of transgenic mice died (Fig. 5C). 50% of transgenic mice survived at 120 h, the longest time-point analyzed. Collectively these data support the hypothesis that SP-B^N confers resistance to infection by *P. aeruginosa*.

Increased expression of SP-B^N in transgenic mice enhances bacterial clearance and survival following infection with S. aureus

In order to determine if SP-B^N also protected against a Gram-positive bacterium, WT and transgenic mice were intranasally inoculated with *S. aureus* and bacterial burden assessed after 8, 24, and 48 h (Fig. 6A). Over-expression of SP-B^N modestly, but significantly enhanced bacterial killing at 8 and 24 h after infection, consistent with an early protective effect of SP-B^N. Intranasal inoculation with a larger dose of *S. aureus* (5×10^8 CFU) resulted in death of 50% of WT mice 48 h after infection (Fig. 6B). There were no more deaths in either group after 48 h. These results indicate that over-expression of SP-B^N modestly protected against airway colonization by *S. aureus*.

DISCUSSION

The 200 amino acid propeptide of SP-B was previously shown to be required for intracellular trafficking of the hydrophobic, membranolytic, mature peptide (6,23,24). The results of the current study suggest that the propeptide also encodes an antimicrobial peptide, herein referred to as SP-B^N, that encompasses an ~81 residue saposin-like domain (Fig. 1C). Unlike the hydrophobic, mature peptide, SP-B^N did not partition with surfactant lipids but was recovered in the BALF supernatant. Recombinant SP-B^N directly killed bacteria, but only at acidic pH, inconsistent with extracellular, alveolar antimicrobial activity. However, SP-B^N indirectly promoted uptake and killing of bacteria by macrophage cell lines *in vitro* and strongly localized to alveolar macrophages *in vivo*. Elevated concentration of SP-B^N in the airspaces of transgenic mice was associated with decreased bacterial load and enhanced survival, particularly following intranasal infection with *Pseudomonas aeruginosa*. IgG directed against SP-B^N specifically inhibited the antimicrobial activity of native SP-B^N in BALF. Thus constitutive expression of the SP-B proprotein may contribute to innate host defense of the alveolar

airspaces via SP-B^N in addition to its vital role in surfactant function mediated by the mature peptide.

The transgenic mice used in this study express a truncated form of the human SP-B proprotein (SP-$B^{\Delta C}$) in alveolar type II epithelial cells but not in non-ciliated bronchiolar cells (19). This observation indicates that the source of SP-B^N is type II cells in transgenic mice but does not exclude a contribution by Clara cells in WT mice. Expression of the SP-$B^{\Delta C}$ transgene in type II cells leads to an approximately 3-fold increase in both SP-B^N and SP-B mature peptide in the airspaces. Although it is possible that the mature peptide contributes to the antimicrobial effect of SP-B in transgenic mice, we believe that this is unlikely. Purified, non-lipid-associated mature SP-B is a potent membranolytic (5–7) and antimicrobial (25,26) peptide; however, mature SP-B non-selectively disrupted both prokaryotic and eukaryotic membranes and, importantly, this activity and its antimicrobial activity, was completely blocked in the presence of surfactant lipids (26). Mature SP-B is always lipid-associated whereas SP-B^N does not associate with surfactant lipids in the airspaces; further, SP-B^N localizes to lysosmes in phagocytic cells and directly kills bacteria at acidic pH. Taken together, these data suggest that SP-B^N promotes macrophage-mediated killing of bacteria in the alveolar airspaces.

We have previously reported that mice expressing the SP-$B^{\Delta C}$ transgene were not protected following infection with a lower dose (1×10^7) of *Pseudomonas aeruginosa* (20). In the current study, a significant protective effect and survival benefit was associated with expression of the transgene following infection with a higher dose (3.7×10^7) of *Pseudomonas aeruginosa*. Bacterial clearance and survival of transgenic mice were also modestly, but significantly, increased following infection with *S. aureus*. These results are similar to a recent study in which constitutive overexpression of cathelicidin in transgenic mice conferred protection against bacterial skin infection (27). Taken together, these findings suggest that exogenous administration of SP-B^N may be of therapeutic benefit.

Unlike the vast majority of antimicrobial peptides that are cationic (28), SP-B^N has a net negative charge: Endogenous mouse SP-B^N has a net negative charge of -2 and human SP-B^N has a negative charge of -6 at neutral pH. The antimicrobial database (29) currently lists 1034 antibacterial peptides of which only 68 are anionic. The anionic character of SP-B^N may confer a significant advantage over cationic antimicrobial peptides in the alveolar environment. Pulmonary surfactant is rich in anionic phospholipids, principally phosphatidylglycerol, which can serve as a sink for cationic peptides; for example, the bactericidal activity of two cathelicidins was inhibited by surfactant phospholipids (30). In contrast, SP-B^N does not bind surfactant lipids at neutral pH and thus escapes sequestration in the airspaces. The association of SP-B^N with bacterial membranes and its bactericidal activity is dramatically increased only in an acidic environment.

SP-B^N shares some features with dermacidin, an anionic, antimicrobial peptide secreted into sweat (31). In addition to a net negative charge (−1 for dermacidin), both peptides are constitutively expressed. However, with respect to structure and function, SP-B^N is most similar to the cytolytic peptides of *Entamoeba histolytica* (14). Amoeba ingests bacteria and kills them in acidic phagolysosomes via the action of the cytolytic peptides, amoebapore A, B, and C. Amoebapore B and C exhibit optimal antibacterial activity in the acidic range and very little activity above pH 6.0 (32,33), unlike dermacidin which is active over a broad pH range (31). Mouse SP-B^N is 24% identical to amoebapore B and 21% identical to amoebapore C; amoebapore B and C share 35% identity. Importantly, SP-B^N and the amoebapore peptides belong to the SAPLIP family of proteins and are predicted to have very similar secondary structures. The three-dimensional structure of amoebapore A was solved by NMR and showed that amoebapore A contains five helices connected by three disulfide bonds (34). Mouse SP-B^N is predicted to contain four amphipathic helices (residues L6-K22, A25-I40, V47-S67, and

P70-V77) and three disulfide bridges arising from 6 invarient cysteine residues. This so-called "saposin-fold" confers resistance to denaturation and proteolysis, likely promoting protein stability/antimicrobial activity in an acidic environment (11,14,35).

Although the findings of this study support the hypothesis that SP-B^N plays an important role in innate defense of the airspaces, a number of questions remain unanswered. First, the mechanism by which SP-B^N kills bacteria is not known. Amoebapores form a stable transmembrane pore that disrupts the cytoplasmic membrane ultimately leading to cell death (32). Given the striking similarities between SP-B^N and amoebapores, it is possible that SP-B^N also depolarizes membranes via formation of pores. Second, the range of SP-B^N cytolytic activity is unclear. Mature SP-B peptide (SP-B, Fig. 1A) displays potent cytolytic activity toward eukaryotic cells that is completely inhibited in the presence of surfactant phospholipids (26). It is possible that SP-B^N may also be cytolytic for eukaryotic cells but that this activity is only unmasked in an acidic environment thus protecting alveolar cells. Third, the spectrum of SP-B^N microbicidal activity remains to be defined: Only representative Gram-positive and Gram-negative organisms were tested in this study. Whether the protective effect of SP-B^N extends broadly to other bacteria remains to be determined. Fourth, the mechanism by which SP-B^N promotes phagocytosis of bacteria by macrophages in culture and the relevance of this activity to clearance of pathogens from the airspaces is still unclear. Finally, the SP-B proprotein contains another saposin-like domain (SP-B^C, Fig. 1A) that has yet to be assessed for potential antimicrobial properties. Overall, based on the results of *in vitro* and *in vivo* studies, we conclude that SP-B^N contributes to innate defense of the lung by supplementing the non-oxidant antimicrobial defenses of alveolar macrophages.

Supplementary Material

Refer to Web version on PubMed Central for supplementary material.

Acknowledgments

The authors thank Ann Maher for excellent secretarial assistance.

References

1. Clark JC, Wert SE, Bachurski CJ, Stahlman MT, Stripp BR, Weaver TE, Whitsett JA. Targeted disruption of the surfactant protein B gene disrupts surfactant homeostasis, causing respiratory failure in newborn mice. Proc Natl Acad Sci USA 1995;92:7794–7798. [PubMed: 7644495]
2. Melton KR, Nesslein LL, Ikegami M, Tichelaar JW, Clark JC, Whitsett JA, Weaver TE. SP-B deficiency causes respiratory failure in adult mice. Am J Physiol: Lung Cell Mol Physiol 2003;285:L543–L549. [PubMed: 12639841]
3. Nogee LM, DeMello DE, Dehner LP, Colten HR. Deficiency of pulmonary surfactant protein B in congenital alveolar proteinosis. N Engl J Med 1993;328:406–410. [PubMed: 8421459]
4. Nogee LM, Garnier G, Dietz HC, Singer L, Murphy AM, Demello DE, Colten HR. A mutation in the surfactant protein B gene responsible for fatal neonatal respiratory disease in multiple kindreds. J Clin Invest 1994;93:1860–1863. [PubMed: 8163685]
5. Ryan MA, Qi XY, Serrano AG, Ikegami M, Perez-Gil J, Johansson J, Weaver TE. Mapping and analysis of the lytic and fusogenic domains of surfactant protein B. Biochemistry 2005;44:861–872. [PubMed: 15654742]
6. Shiffer K, Hawgood S, Duzgunes N, Goerke J. Interactions of the low molecular weight group of surfactant-associated proteins (SP 5–18) with pulmonary surfactant lipids. Biochemistry 1988;27:2689–2695. [PubMed: 3401444]
7. Oosterlaken-Dijksterhuis MA, Van Eijk M, Van Golde LMG, Haagsman HP. Lipid mixing is mediated by the hydrophobic surfactant protein SP-B but not by SP-C. Biochim Biophys Acta 1992;1110:45–50. [PubMed: 1390835]

8. Poulain FR, Allen L, Williams MC, Hamilton RL, Hawgood S. Effects of surfactant apolipoproteins on liposome structure - implications for tubular myelin formation. Am J Physiol 1992;262:L730–L739. [PubMed: 1616057]
9. Patthy L. Homology of the precursor of pulmonary surfactant-associated protein SP-B with prosaposin and sulfated glycoprotein-1. J Biol Chem 1991;266:6035–6037. [PubMed: 1688355]
10. Bruhn H. A short guided tour through functional and structural features of saposin-like proteins. Biochem J 2005;389:249–257. [PubMed: 15992358]
11. Liepinsh E, Andersson M, Ruysschaert JM, Otting G. Saposin fold revealed by the NMR structure of NK-lysin. Nat Struct Biol 1997;4:793–795. [PubMed: 9334742]
12. Whitsett JA, Weaver TE. Mechanisms of disease: Hydrophobic surfactant proteins in lung function and disease. N Engl J Med 2002;347:2141–2148. [PubMed: 12501227]
13. Weaver TE, Conkright JJ. Function of Surfactant Proteins B and C. Annu Rev Physiol 2001;63:555–578. [PubMed: 11181967]
14. Leippe M. Antimicrobial and cytolytic polypeptides of amoeboid protozoa--effector molecules of primitive phagocytes. Dev Comp Immunol 1999;23:267–279. [PubMed: 10426421]
15. Akinbi HT, Epaud R, Bhatt H, Weaver TE. Bacterial killing is enhanced by expression of lysozyme in the lungs of transgenic mice. J Immunol 2000;165:5760–5766. [PubMed: 11067934]
16. Nesslein LL, Melton KR, Ikegami M, Na CL, Wert SE, Rice WR, Whitsett JA, Weaver TE. Partial SP-B deficiency perturbs lung function and causes air space abnormalities. Am J Physiol: Lung Cell Mol Physiol 2005;288:L1154–L1161. [PubMed: 15722377]
17. Vunta H, Davis F, Palempalli UD, Bhat D, Arner RJ, Thompson JT, Peterson DG, Reddy CC, Prabhu KS. The anti-inflammatory effects of selenium are mediated through 15-deoxy-Delta12,14-prostaglandin J2 in macrophages. J Biol Chem 2007;282:17964–17973. [PubMed: 17439952]
18. Shibata Y, Berclaz PY, Chroneos ZC, Yoshida M, Whitsett JA, Trapnell BC. GM-CSF regulates alveolar macrophage differentiation and innate immunity in the lung through PU.1. Immunity 2001;15:557–567. [PubMed: 11672538]
19. Akinbi HT, Breslin JS, Ikegami M, Iwamoto HS, Clark JC, Whitsett JA, Jobe AH, Weaver TE. Rescue of SP-B knockout mice with a truncated SP-B proprotein - Function of the C-terminal propeptide. J Biol Chem 1997;272:9640–9647. [PubMed: 9092492]
20. Akinbi HT, Bhatt H, Hull WM, Weaver TE. Altered surfactant protein B levels in transgenic mice do not affect clearance of bacteria from the lungs. Pediatr Res 1999;46:530–534. [PubMed: 10541314]
21. Johansson J, Jornvall H, Curstedt T. Human surfactant polypeptide SP-B -disulfide bridges, C-terminal end, and peptide analysis of the airway form. FEBS Lett 1992;301:165–167. [PubMed: 1568474]
22. Johansson J, Curstedt T, Jornvall H. Surfactant protein-B - disulfide bridges, structural properties, and kringle similarities. Biochemistry 1991;30:6917–6921. [PubMed: 1648964]
23. Lin S, Phillips KS, Wilder MR, Weaver TE. Structural requirements for intracellular transport of pulmonary surfactant protein B (SP-B). Biochim Biophys Acta 1996;1312:177–185. [PubMed: 8703986]
24. Lin S, Akinbi HT, Breslin JS, Weaver TE. Structural requirements for targeting of surfactant protein B (SP-B) to secretory granules in vitro and in vivo. J Biol Chem 1996;271:19689–19695. [PubMed: 8702672]
25. Kaser MR, Skouteris GG. Inhibition of bacterial growth by synthetic SP-B1-78 peptides. Peptides 1997;18:1441–1444. [PubMed: 9392848]
26. Ryan MA, Akinbi HT, Serrano AG, Perez-Gil J, Wu HX, McCormack FX, Weaver TE. Antimicrobial activity of native and synthetic surfactant protein B peptides. J Immunol 2006;176:416–425. [PubMed: 16365435]
27. Lee PH, Ohtake T, Zaiou M, Murakami M, Rudisill JA, Lin KH, Gallo RL. Expression of an additional cathelicidin antimicrobial peptide protects against bacterial skin infection. Proc Natl Acad Sci U S A 2005;102:3750–3755. [PubMed: 15728389]
28. Brown KL, Hancock REW. Cationic host defense (antimicrobial) peptides. Curr Opin Immunol 2006;18:24–30. [PubMed: 16337365]

29. Wang Z, Wang G. APD: the Antimicrobial Peptide Database. Nucleic Acids Res 2004;32:D590–D592. [PubMed: 14681488]

30. Wang Y, Walter G, Herting E, Agerberth B, Johansson J. Antibacterial activities of the cathelicidins prophenin (residues 62 to 79) and LL-37 in the presence of a lung surfactant preparation. Antimicrob Agents Chemother 2004;48:2097–2100. [PubMed: 15155206]

31. Schittek B, Hipfel R, Sauer B, Bauer J, Kalbacher H, Stevanovic S, Schirle M, Schroeder K, Blin N, Meier F, Rassner G, Garbe C. Dermcidin: a novel human antibiotic peptide secreted by sweat glands. Nat Immunol 2001;2:1133–1137. [PubMed: 11694882]

32. Leippe M, Ebel S, Schoenberger OL, Horstmann RD, Muller-Eberhard HJ. Pore-forming peptide of pathogenic Entamoeba histolytica. Proc Natl Acad Sci U S A 1991;88:7659–7663. [PubMed: 1881907]

33. Bruhn H, Riekens B, Berninghausen O, Leippe M. Amoebapores and NK-lysin, members of a class of structurally distinct antimicrobial and cytolytic peptides from protozoa and mammals: a comparative functional analysis. Biochem J 2003;375:737–744. [PubMed: 12917014]

34. Moos MJ, Nguyen NY, Liu TY. Reproducible high yield sequencing of proteins electrophoretically separated and transferred to an inert support. J Biol Chem 1988;263:6005–6008. [PubMed: 3360771]

35. Andersson M, Curstedt T, Jornvall H, Johansson J. An amphipathic helical motif common to tumourolytic polypeptide NK-lysin and pulmonary surfactant polypeptide SP-B. FEBS Lett 1995;362:328–332. [PubMed: 7729523]

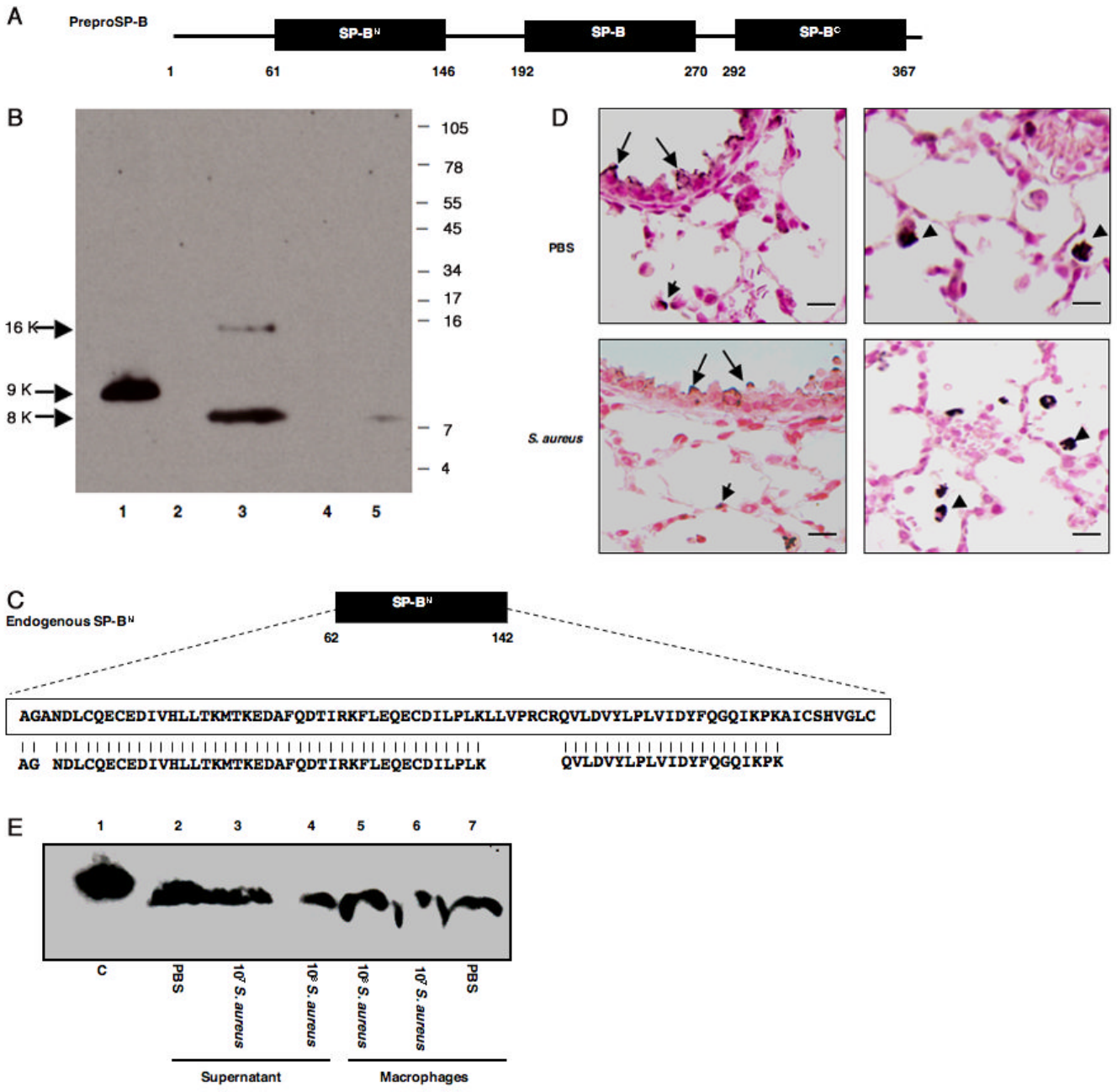

Figure 1. Identification of endogenous SP-B^N in mouse lung

A. Schematic representation of preproSP-B protein. The boxes indicate the predicted location of three saposin-like domains in mouse preproSP-B: N-terminal peptide (SP-B^N) residues 61 through 146, mature peptide (SP-B), residues 192-270, and C-terminal peptide (SP-B^C), residues 292-367. **B.** Antibody was generated against recombinant mouse SP-B^N (residues 61-146 with a C-terminal hexahistidine tag) and used to detect endogenous SP-B^N (Mr = 8000) by Western blotting of 20 μg mouse BALF. Lane 1, recombinant SP-B^N; Lane 2, mouse liver homogenate; Lane 3, BALF supernatant; Lane 4, blank; Lane 5, BALF surfactant pellet. **C.** Predicted sequence of mouse SP-B^N (boxed upper line). The lower line is sequence derived from MS/MS analyses of tryptic peptides from purified rat SP-B^N. Alanine and glycine were established as the NH_2-terminal residues of endogenous rat SP-B^N by Edman degradation.

D. Lung sections from mice intranasally challenged with PBS (upper panels) or *S. aureus* (lower panels) were immunostained with SP-B^N antibody. SP-B^N was detectedin bronchiolar epithelial cells (left panels, arrows), type II epithelial cells (left panels, short arrows) and macrophages (right panels, arrow heads). Double immunofluorescent staining (not shown) demonstrated that most cells in the airspaces airspaces were positive for the macrophage marker mac-3^+ and negative for the neutrophil marker Ly-$6G^-$. Subsequent experiments thus focused to macrophages. Scale bar = 50 μm. **E.** SP-B^N antibody detected endogenous SP-B^N (Mr = 8000) in mouse lung BALF supernatant and cell pellet isolated from uninfected mice or 24h after inoculation with 10^7 or 10^8 CFU *S. aureus*. Lane 1, recombinant SP-B^N; lane 2, BALF supernatant from uninfected mice; lanes 3 and 4, BALF supernatant after infection; lanes 5 and 6, cell pellets isolated from BALF following infection; lane 7, cell pellet isolated from BALF of uninfected mice.

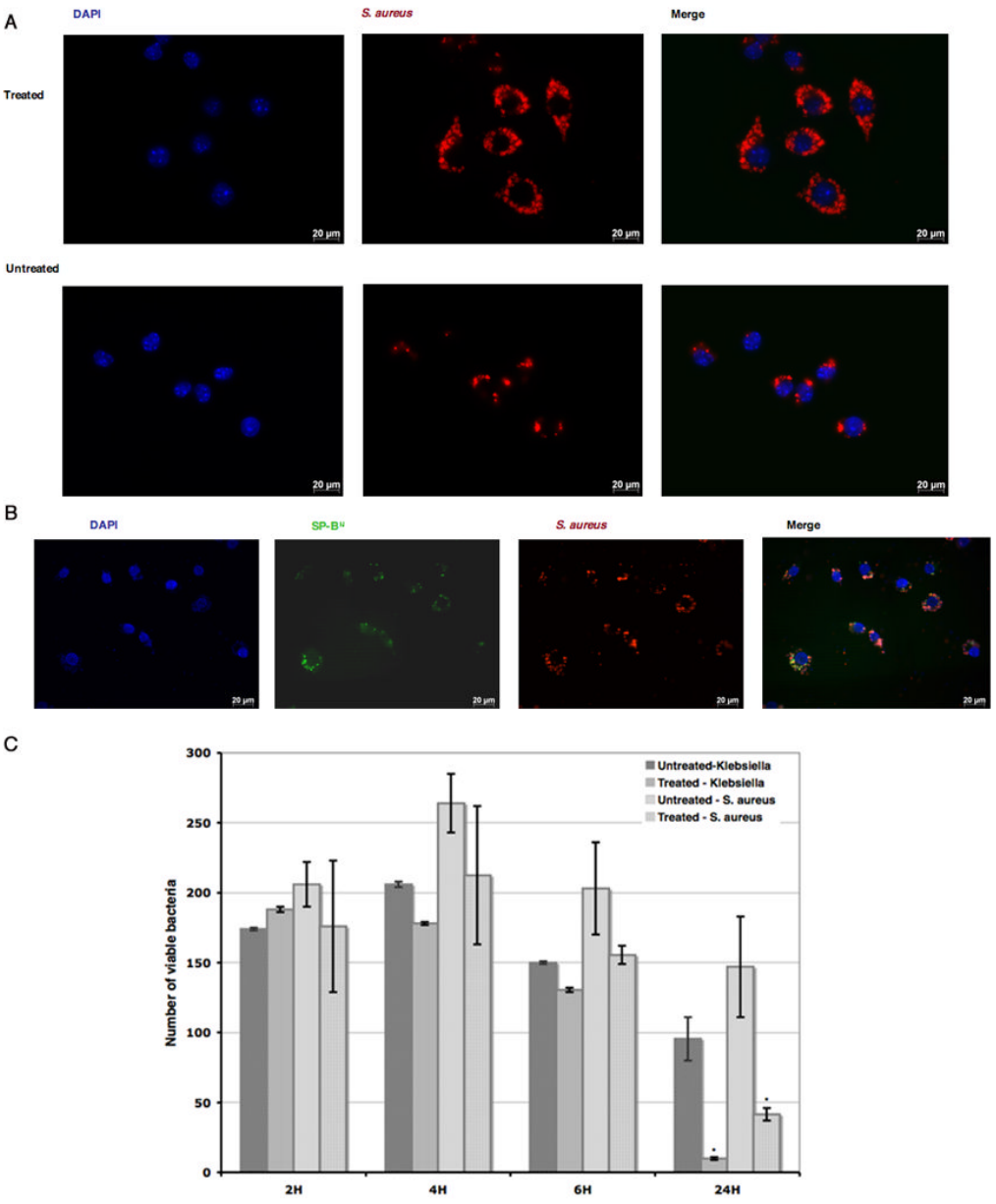

Figure 2. SP-B^N is internalized by RAW264.7 cells resulting in increased uptake of bacteria and killing activity

A. RAW264.7 cells were preincubated with (treated, upper panel) or without (untreated, lower panel) 18 μg/ml of recombinant SP-B^N for 1h. Cells were washed twice with warm PBS buffer to remove SP-B^N and heat-killed, Alexa fluorescent-labeled *S. aureus* were added to the media for 1h. DAPI (nuclear stain) was added to the mounting reagent. Bacterial uptake was assessed by fluorescence microscopy. **B.** RAW264.7 cells were preincubated for 1h with 36μg/ml of FITC-labeled SP-B^N followed by incubation with heat-killed *S. aureus* (Alexa Fluor 594) for 1h, as described in A, above. Subcellular localization of SP-B^N and bacteria was assessed by fluorescence microscopy. **C.** RAW264.7 cells were preincubated with recombinant SP-B^N for 1h. Cells were washed twice with PBS and *S. aureus (*1.5×10^6 CFU) or *K. pneumoniae* (1×10^6 CFU) was added to the media. After an additional hour, the media was replaced and 100 μg/ml carbenicillin or gentamycin was added to kill extracellular *S. aureus or K.*

pneumoniae. Cells were lysed with 1% triton X-100 at the indicated time points after infection and the number of viable bacteria was assessed by quantitative culture of cell lysates. Data represent mean ± SEM of three independent experiments; *, p =0.007 vs. untreated RAW264.7 cells at 24h post-infection.

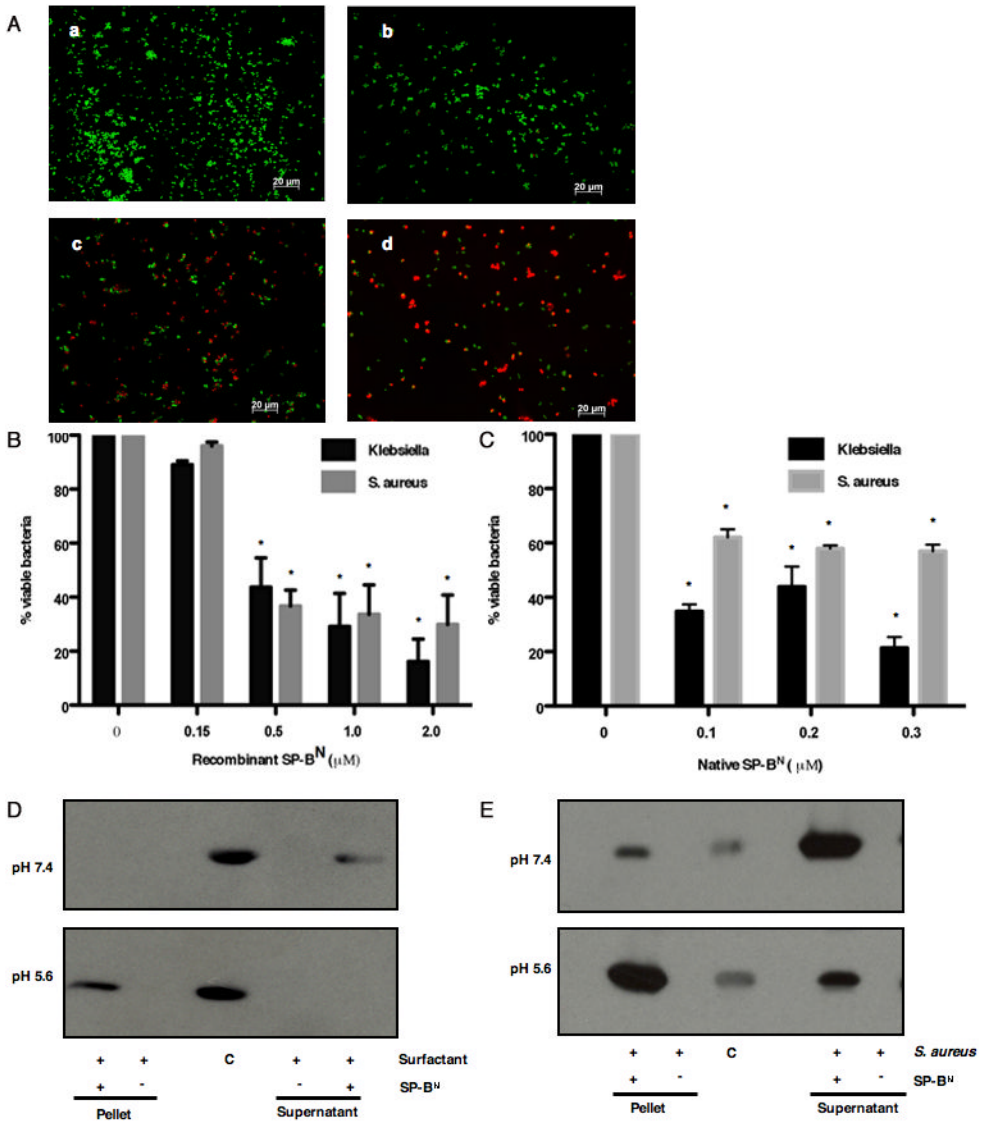

Figure 3. SP-B^N directly kills *S. aureus or K. pneumoniae* at acidic pH

A. *S. aureus* (OD600 = 0.1) was incubated without (panel a) or with 5 μg (panel c) or 10 μg (panels b and d) recombinant SP-B^N for 90 minutes at 37°C. Bacteria were suspended in buffer, pH 7.4 (panel b) or pH 5.6 (panel a, c, and d) and stained with the vital dye Syto9 (stains living bacteria green) and propidum iodide (stains dead/dying bacteria red) followed by fluorescence microscopy to assess viability. **B.** Increasing amounts of recombinant SP-B^N were added to 10^3 CFU of *S. aureus* (grey bars) or *K. pneumoniae* (Black bars) suspended in 100 μl of 2 mM sodium acetate buffer, pH 5.6, and incubated for 3 h at 37°C. The number of viable bacteria were assessed by quantitative culture and results expressed as the mean ± SEM of three independent experiments; *, $p < 0.05$ vs. untreated (0 μM) group. **C**. Purified native rat SP-B^N was added to 10^3 CFU of *S. aureus* (grey bars) or *K. pneumoniae* (Black bars) suspended in 100 μl of 2 mM sodium acetate buffer, pH 5.6, and incubated for 3 h at 37°C. The number of viable bacteria was assessed by quantitative culture and results expressed as the mean ± SEM of three independent experiments; *, $p < 0.05$ vs. untreated (0 μM) group. **D.** 10 μg recombinant SP-B^N was added to mouse BALF at pH 7.4 (upper panel) or pH 5.6 (lower panel), incubated at RT for 2 h then centrifuged to separate surfactant lipids and supernatant.

Supernatants and lipid pellets were analyzed by SDS-PAGE/western blotting with SP-B^N antibody. **E.** 10^5 CFU of *S. aureus* was suspended in buffer, pH 7.4 or pH 5.6, incubated with 10 μg recombinant SP-B^N for 2 hrs at RT, centrifuged to separate the bacterial pellet and supernatant and analyzed as in panel d. C, 0.1μg recombinant SP-B^N loaded as positive control.

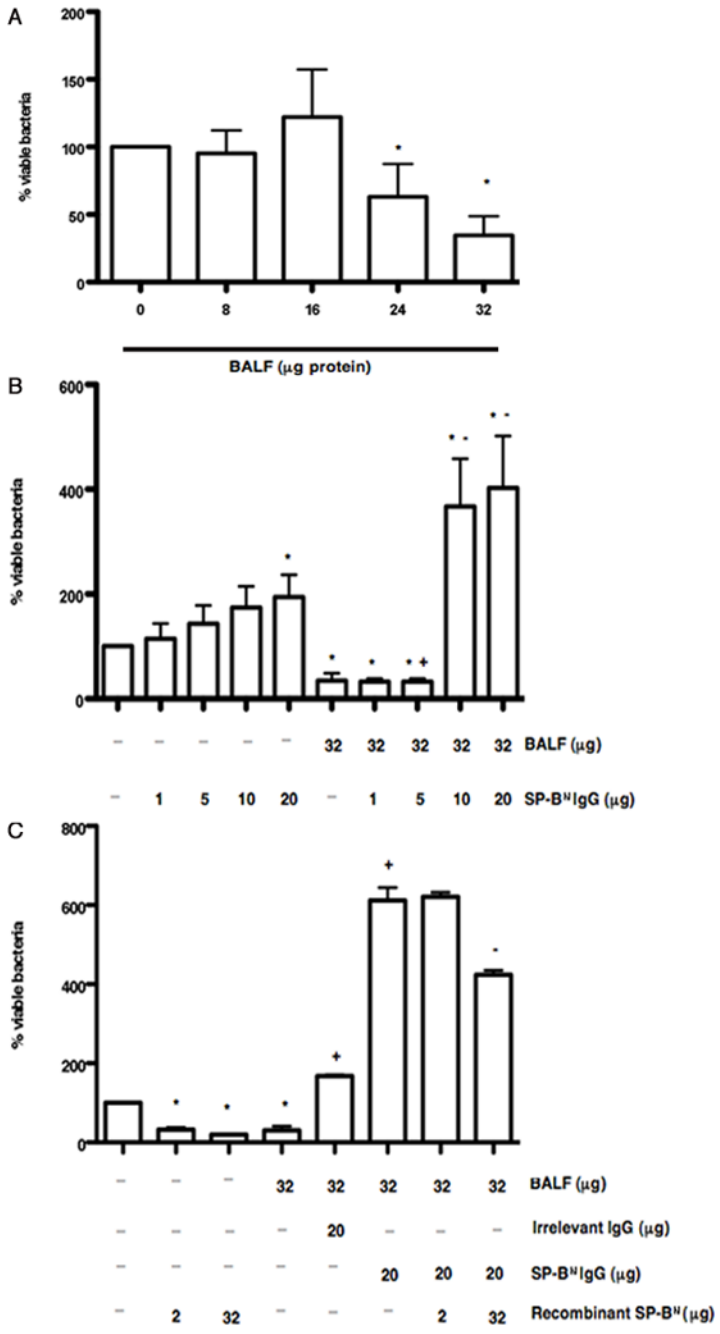

Figure 4. Native SP-B^N in BALF inhibits growth of *P. aeruginosa*

A. BALF supernatant (containing 8–32 μg protein) was added to 10^7 CFU of bioluminescent *P. aeruginosa Xen 5* suspended in 100 μl of 2 mM sodium acetate buffer, pH 5.6, and incubated overnight at 37°C. The number of viable bacteria was assessed by measuring luminescence. Results are expressed as mean ± SEM of three independent experiments; *, $p<0.05$ vs. buffer (0 μg BALF). **B**. 1×10^7 CFU of *P. aeruginosa* in 100 μl of 2 mM sodium acetate buffer, pH 5.6, was incubated with IgG (0–20 μg) directed against SP-B^N and/or 32 μg of BALF supernatant. The number of viable bacteria was assessed by measuring luminescence. Results are expressed as mean ± SEM of three independent experiments; *, $p<0.05$ vs. buffer (0 μg BALF); +, $p = 0.004$ vs. 32 μg BALF; -, $p<0.0001$ vs. 32 μg BALF. **C.** 1×10^7 CFU of

bioluminescent *P. Aeruginosa* Xen 5 in 100 μl of 2 mM sodium acetate buffer, pH 5.6, were incubated with recombinant SP-B^N, BALF supernatant or BALF + irrelevant IgG or SP-B^N IgG as described in B; additional recombinant SP-B^N was added to determine if the inhibitory effect of SP-B^N IgG could be reversed. The number of viable bacteria was assessed by measuring luminescence. Results are expressed as mean ± SEM of three independent experiments; *, $p<0.05$, vs. buffer (0 μg BALF); +, $p< 0.001$ vs. 32 μg BALF; -, $p=0.02$ vs. 32 μg BALF + 20 μg IgG.

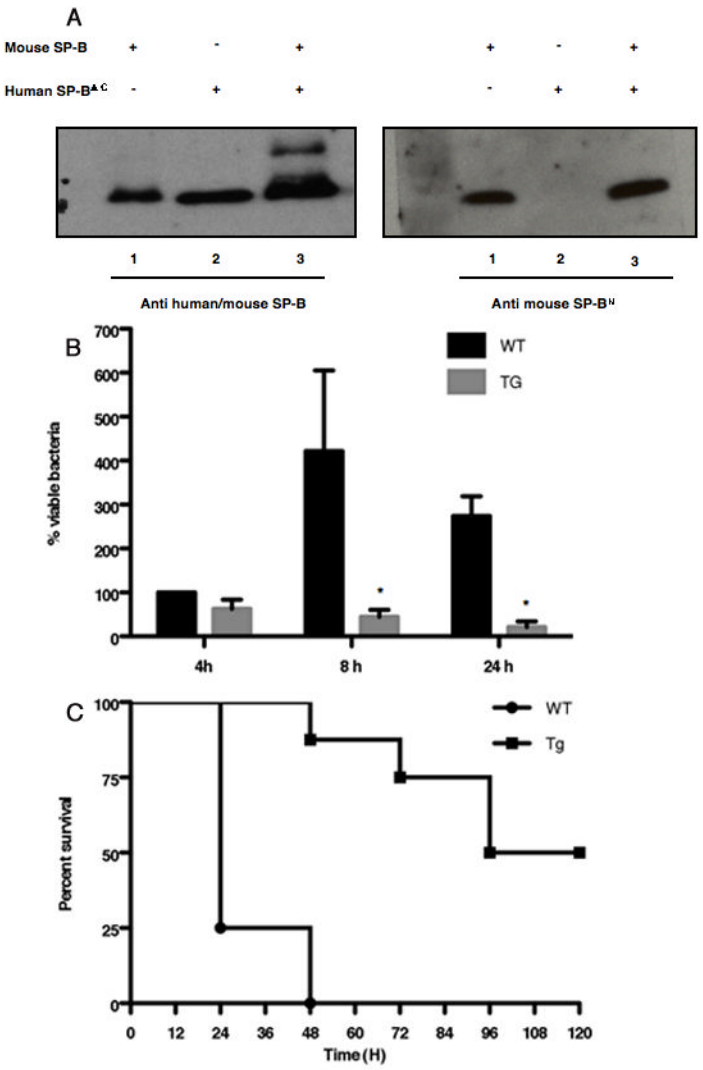

Figure 5. Increased expression of SP-B^{N} in transgenic mice enhances bacterial clearance and survival following infection with *P. aeruginosa*

A. The concentration of SP-B^{N} in the airspaces was assessed in 3 groups of mice: WT mice (lane 1), transgenic mice expressing truncated human SP-B proprotein (SP-B ^{C}) in the mouse SP-B$^{-/-}$ background (hSP-B$^{\Delta C}$/mSP-B$^{-/-}$, lane 2), and transgenic mice expressing SP-B$^{\Delta C}$ in the WT background (hSP-B$^{\Delta C}$/mSP-B$^{+/+}$, lane 3). 20 μg of BALF supernatant was fractionated by SDS-PAGE under nonreducing (left panel) or reducing conditions (right panel), blotted onto nitrocellulose, and incubated with antibody that detects both human and mouse SP-B (23) (left panel) or mouse-specific SP-B^{N} antibody (right panel). **B.** Transgenic (hSP-B$^{\Delta C}$/mSP-B$^{+/+}$) and WT mice were intranasally inoculated with 3.7×10^{7} CFU of bioluminescent *P. aeruginosa* Xen 5. *In vivo* bioluminescence was assessed under anesthesia at 1, 8, and 24 h post-infection and quantitative analysis of bioluminescence of mice. Values are means ± SEM; The experiments were repeated 3 times and data pooled, n=12–15 mice/group per time point. *, P=0.01, transgenic vs. WT mice. **C.** Survival after intranasal instillation of *P. aeruginosa* Xen 5. Transgenic or WT mice (n=16 for each genotype) were infected by intranasal instillation of 3.7×10^{7} CFU of *P. aeruginosa* Xen 5. The number of surviving mice was documented every 12h until 120 hours after infection. *, P<0.001, transgenic vs. WT mice.

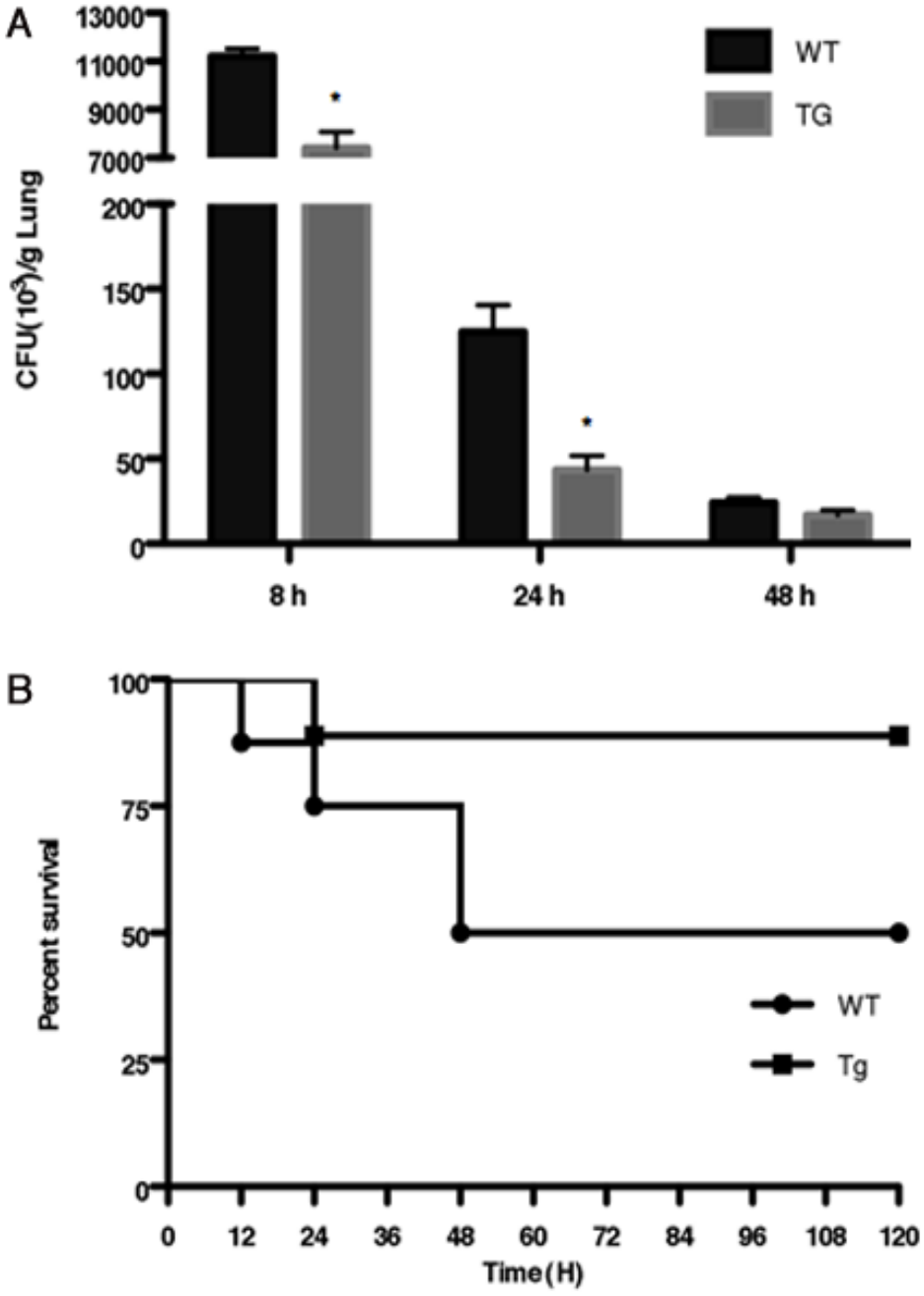

Figure 6. Increased expression of SP-B^N in transgenic mice enhances survival and bacterial clearance following infection with *S. aureus*

A. Lung bacterial burden was assessed by quantitative culture of lung homogenates at 8, 24 or 48 h after intranasal instillation of 2×10^8 CFU of *S. aureus*. N=4 mice/group per time point. The experiments were repeated 3 times and data pooled. *, P<0.001, transgenic vs. WT mice. **B.** Survival after intranasal instillation of *S. aureus*. Transgenic or WT mice (n=16 for each genotype) were infected by intranasal inoculation of 5×10^8 CFU of *S. aureus*; the number of surviving mice was documented every 12h until 120 hours after infection. *, P<0.05, transgenic vs. WT mice.